NIH Public Access
Author Manuscript
J Proteome Res. Author manuscript; available in PMC 2010 April 26.

Published in final edited form as:
J Proteome Res. 2010 March 5; 9(3): 1496–1509. doi:10.1021/pr901024z.

Region-Specific Protein Abundance Changes in the Brain of MPTP-induced Parkinson's Disease Mouse Model

Xu Zhang[‡,*], **Jianying Zhou**[‡,*], **Mark H. Chin**[§], **Athena A. Schepmoes**[‡], **Vladislav A. Petyuk**[‡], **Karl K. Weitz**[‡], **Brianne O. Petritis**[‡], **Matthew E. Monroe**[‡], **David G. Camp II**[‡], **Stephen A. Wood**[$], **William P. Melega**[§], **Diana J. Bigelow**[‡], **Desmond J. Smith**[§], **Wei-Jun Qian**[‡,§§], and **Richard D. Smith**[‡]

[‡]Biological Sciences Division and Environmental Molecular Sciences Laboratory, Pacific Northwest National Laboratory, P.O Box 999, Richland, WA 99352

[§]Department of Molecular and Medical Pharmacology, UCLA School of Medicine, P.O. Box 951735, Los Angeles, CA 90095

[$]National Centre for Adult Stem Cell Research, Griffith University, Nathan, Queensland, 4111, Australia.

SUMMARY

Parkinson's disease (PD) is characterized by dopaminergic neurodegeneration in the nigrostriatal region of the brain; however, the neurodegeneration extends well beyond dopaminergic neurons. To gain a better understanding of the molecular changes relevant to PD, we applied two-dimensional LC-MS/MS to comparatively analyze the proteome changes in four brain regions (striatum, cerebellum, cortex, and the rest of brain) using a MPTP-induced PD mouse model with the objective to identify nigrostriatal-specific and other region-specific protein abundance changes. The combined analyses resulted in the identification of 4,895 non-redundant proteins with at least two unique peptides per protein. The relative abundance changes in each analyzed brain region were estimated based on the spectral count information. A total of 518 proteins were observed with significant MPTP-induced changes across different brain regions. 270 of these proteins were observed with specific changes occurring either only in the striatum and/or in the rest of the brain region that contains substantia nigra, suggesting that these proteins are associated with the underlying nigrostriatal pathways. Many of the proteins that exhibit significant abundance changes were associated with dopamine signaling, mitochondrial dysfunction, the ubiquitin system, calcium signaling, the oxidative stress response, and apoptosis. A set of proteins with either consistent change across all brain regions or with changes specific to the cortex and cerebellum regions were also detected. One of the interesting proteins is ubiquitin specific protease (USP9X), a deubiquination enzyme involved in the protection of proteins from degradation and promotion of the TGF-β pathway, which exhibited altered abundances in all brain regions. Western blot validation showed similar spatial changes, suggesting that USP9X is potentially associated with neurodegeneration. Together, this study for the first time presents an overall picture of proteome changes underlying both nigrostriatal pathways and other brain regions potentially involved in MPTP-induced neurodegeneration. The observed molecular changes provide a valuable reference resource for future hypothesis-driven functional studies of PD.

§§ To whom correspondence should be addressed: Biological Sciences Division and Environmental Molecular Sciences Laboratory, Pacific Northwest National Laboratory, P.O Box 999, Richland, WA 99352. Phone: (509)371-6572; weijun.qian@pnl.gov .
*These authors contributed equally to this work.

NIH-PA Author Manuscript
NIH-PA Author Manuscript
NIH-PA Author Manuscript

NIH-PA Author Manuscript

NIH-PA Author Manuscript

NIH-PA Author Manuscript

Keywords

mass spectrometry; mouse brain proteome; Parkinson's disease; MPTP; LC-MS/MS; mouse model

INTRODUCTION

Parkinson's disease (PD) represents a chronic, progressive neurodegenerative movement disorder characterized by the loss of dopaminergic neurons in the substantia nigra (SN) and accumulation of intraneuronal Lewy body inclusions (1-3). Since the first description of PD in 1817 (4), extensive studies have been made including the identification of 13 PD associated genetic loci (5,6), which provide basic insights into the pathogenesis of the disease. Current hypotheses regarding mechanisms underlying the etiology and pathogenesis of PD, include abnormal protein aggregation, mitochondrial dysfunction, oxidative stress, and failure of the ubiquitin-proteasome system (4), and were mainly derived from studies using postmortem tissues or animal models; most notably, the 1-methyl-4-phenyl-1,2,3,6-tetrahydropyridine (MPTP)-models (7-10). As a selective neurotoxin, MPTP primarily targets the nigrostriatal dopaminergic system via the high affinity dopamine transporter (11,12), where it induces the generation of excessive reactive oxygen species (ROS) and the selective destruction of dopaminergic neurons, thereby decreasing the dopaminergic projection into the striatum (7-10). The MPTP model has become the most commonly used PD model for elucidating molecular cascades of neurodegeneration (7); however, the exact etiology and mechanisms leading to the development of PD still remain unclear. Moreover, the neurodegeneration extends well beyond dopaminergic neurons (7,13). Therefore, identification of MPTP-induced molecular changes within different brain regions is essential for defining molecular mechanisms underlying PD neurodegeneration.

Significant efforts have recently been focused on the application of proteomics technologies in order to profile protein abundance changes in brain tissues and biofluids in patients or animal models of neurodegenerative diseases (14,15). Studies using Two-dimensional electrophoresis (2DE) coupled with mass spectrometry (MS) in PD patients, parkin-deficient mice, as well as MPTP-treated mice have consolidated the view that mitochondrial dysfunction and oxidative stress are involved in PD pathogenesis (16-21). We have also recently applied LC-MS and microarrays to profile protein and transcript abundance changes in the striatum of PD mouse models induced by MPTP and methamphetamine (METH) treatment for the purpose of identifying molecular changes associated with PD (22). However, since most of the studies were limited to only a single brain region, such as substantia nigra or striatum, without comparison with other brain regions, it is unclear whether the observed molecular changes are specific to nigrostriatal pathways. Moreover, the molecular changes in other brain regions may potentially be associated with neurodegeneration in PD have yet to be identified.

In this work we identify spatially resolved proteome changes induced by MPTP by comparatively analyzing four brain regions, i.e., striatum, cerebellum, cortex, and the rest of the brain tissue (ROB). Off-line strong cation exchange (SCX) LC fractionation was coupled with high resolution capillary reversed-phase LC-MS/MS to enhance the overall proteome coverage over the previous single dimensional LC-MS based study (22). The results reveal a total of 518 proteins with significant abundance changes induced by MPTP in the different brain regions; 270 of these proteins show abundance changes specific to the nigrostriatal region. Many of the observed abundance changes are associated with the dopamine signaling pathway, mitochondrial dysfunction, the ubiquitin system, calcium signaling, and apoptosis.

NIH-PA Author Manuscript

NIH-PA Author Manuscript

NIH-PA Author Manuscript

EXPERIMENTAL PROCEDURES

MPTP Mouse Model

Adult C57BL/6J male mice (8 weeks, 21–27 g), obtained from Jackson Laboratories (Bar Harbor, ME), were administrated four intraperitoneal (i.p.) injections of MPTP-HCl (Sigma-Aldrich, St. Louis, MO) in saline (15 mg/kg per injection) at 2 h intervals; the control mice were injected with the same volume of sterilized saline only. The cortex, cerebellum, striatum and rest of brain were dissected from 4 MPTP and 4 control mice 7 days after the injection, and snap-frozen immediately in liquid nitrogen until future processing. Animal procedures were performed in accordance with the National Institutes of Health Guide for the Care and Use of Laboratory Animals. The loss of dopamine in striatum was assessed by using high performance liquid chromatography (HPLC) as previously described (22) and ~88% decrease in striatal dopamine level was observed following the MPTP treatment.

Protein Digestion

All tissues were homogenized in 50 mM NH_4HCO_3 (pH 7.8), and protein concentration was determined by a BCA assay (Pierce, Rockford, IL). Aliquots of homogenates from the same brain region from four mice were pooled for protein digestion. Approximately, 300 μg pooled sample was subsequently treated with 50% (v/v) trifluoroethanol (TFE) (Sigma-Aldrich) for 2 h at 60 °C, 5 mM tributylphosphine (TBP) (Sigma) for 0.5 h at 60 °C, 40 mM iodoacetamide (IAA) for 1 h at 37 °C, and then diluted five-fold with 50 mM NH_4HCO_3 prior to digestion with sequencing-grade trypsin (Promega, Madison, WI) for 3 h at 37 °C at a 1:50 trypsin to protein ratio (w:w) with 1 mM $CaCl_2$ added during the digestion. The digested sample was then cleaned up with a SPE C-18 column (Supelco, Bellefonte, PA), then dried down using a speed-vac concentrator.

Strong Cation Exchange (SCX) Fractionation

The dried peptides were dissolved in 25 mM NH_4HCO_3, and subjected to SCX fractionation using a 200 × 2.1 mm (5 μm particles, 300 Å pore size) Polysulfoethyl A column (PolyLC, Columbia, MD) on an automated HPLC (Agilent, Palo Alto, CA) at a flow rate of 0.2 mL/min. Mobile phase solvents consisted of (A) 10 mM ammonium formate, 25% acetonitrile, pH 3.0 and (B) 500 mM ammonium formate, 25% acetonitrile, pH 6.8. Once the column was loaded, isocratic conditions at 100% A were maintained for 10 min. Peptides were separated applying a gradient from 0 to 50% B over 40 min, followed by a gradient of 50–100% B over 10 min. The gradient was then held at 100% solvent B for another 10 min. Twenty-five fractions were collected for each sample. Following lyophilization, the fractions were dissolved in 25 mM NH_4HCO_3 and stored at −80 °C.

Capillary LC-MS/MS Analysis

Each of the 25 SCX fractions was further analyzed using a fully automated custom-built capillary HPLC system coupled online with an LTQ ion trap mass spectrometer (ThermoFinnigan, San Jose, CA) using an in-house manufactured electrospray ionization interface. The reversed-phase capillary column was slurry packed using 3 μm Jupiter C18 particles (Phenomenex, Torrance, CA) in a 75 μm (inside diameter) × 65 cm fused silica capillary (Polymicro Technologies, Phoenix, AZ). The mobile phases consisted of A (0.2% acetic acid and 0.05% TFA in water) and B (0.1% TFA in 90% acetonitrile). An exponential gradient was employed during the separation, which started with 100% A that gradually increased to 60% B over the course of 100 min. The instrument was operated in data-dependent mode with an m/z range of 400–2000. The five most abundant ions from the MS analysis were selected for MS/MS analysis using a normalized collision energy setting of

NIH-PA Author Manuscript

NIH-PA Author Manuscript

NIH-PA Author Manuscript

35%. Dynamic exclusion was used to avoid repetitive analysis of the same abundant precursor ion.

MS/MS Data Analysis

The MS/MS data were searched against the mouse International Protein Index (IPI) database with a total of 51,252 total protein entries (Version 3.19, released on July 25, 2006, available on-line at http://www.ebi.ac.uk/IPI) with the decoy database searching option (for assessing false positive rate) using X!Tandem 2 software (23). The search parameters used were: 3 Da tolerance for precursor ion masses and 1 Da for fragment ion masses with no enzyme restraint and a maximum of three missed tryptic cleavages. Modifications for the static carboxamidomethylation of cysteine and dynamic oxidation of methionine were applied during the database search.

The following criteria were used for initial filtering of the raw X!Tandem results: Peptide_Expectation_Value_Log(e) < −2 with partial or full tryptic cleavage. Such criteria were established for mouse brain tissue using sequence-reversed database searching that provides 3.7% of false positive peptide identifications at the final identified unique peptide level (24). The reversed human protein database was created by reversing the order of the amino acid sequences for each protein, and the false positive rate (FPR) for peptide identifications was estimated by dividing the number of unique peptides identified from the reversed database search (N_R) by the number of unique peptides identified from the normal database search (N_N), i.e. FPR = N_R/N_N.

To remove redundant protein entries, ProteinProphet™ software (v1.7) was used as a clustering tool to group similar or related protein entries into protein groups (25). Peptides that passed the filtering criteria were assigned the identical probability score of 1 and entered into the software program (done exclusively for cluster analysis) to generate a final list of non-redundant proteins/protein groups. One protein IPI number was randomly selected to represent each corresponding protein group that consists of a number of database entries. Only those proteins or protein groups with two or more unique peptide identifications were considered to be confident protein identifications.

Abundance ratios of proteins were calculated based on the spectral count of proteins from each region in the format of fold-changes, i.e., if abundance ratio of [MPTP]/[Ctrl] ≥1, fold change equals [MPTP]/[Ctrl]-1, and if abundance ratio of [MPTP]/[Ctrl] <1, fold change equals 1-[Ctrl]/[MPTP]. To identify statistically significant abundance changes, proteins identified from the analyses for each brain region were divided into three groups based on their relative abundance levels: the high-abundance group (mean spectral count between two biological conditions greater than 10); the medium-abundance group (mean spectral count between 5 and 10); and the low-abundance group (mean spectral count less than 5), similar to the method previously described (26). Standard deviations (σ) of fold-changes between two replicate 2D-LC-MS/MS analyses were calculated for each protein abundance group based on the data from the previous study (26) . A fold change greater than 4σ was required for a protein to be considered to be significant for each protein group. The final cutoffs of fold-changes are 5, 1.75, and 0.6 for the low-, medium-, and high-abundance groups, respectively. Only those proteins with total spectral counts of peptide observation above 5 were retained for the analysis of abundance changes.

Western Blot Verifications of Selected Proteins

15 μg proteins were separated on a 4-12% NuPAGE Novex Bis-Tris gel (1 mm thick, Invitrogen, CA), and transferred to a 0.2 uL Nitrocellulose membrane (Invitrogen). The membranes were blocked in 10% nonfat milk in Tris-buffered saline (TBS: 50 mM Tris, 150

NIH-PA Author Manuscript

NIH-PA Author Manuscript

NIH-PA Author Manuscript

mM NaCl, pH 7.4) at room temperature for one hour, followed by different primary and secondary antibody incubations. Antibodies were used at the following dilutions: Beta tubulin (mouse, Abcam, MA), 1:20000; Usp9x (rabbit, provided by Dr. Stephen Wood (27)), 1:2000; Atp6v1f (Rabbit, Santa Cruz Biotechnology, CA), 1:200; Goat anti-rabbit IgG – HRP (Invitrogen), 1:5000; Rabbit anti-mouse HRP-IgG (Pierce), 1:20000. Immunoblotting bands were detected by Lumi-Imager F1 (Boehringer Mannheim Corporation, Indianapolis, IN).

RESULTS

LC-MS/MS Profiling of Four Brain Regions

To achieve in-depth proteome coverage of the mouse brain regions, we applied offline SCX fractionation coupled with high resolution capillary reversed-phase LC-MS/MS for comparative analyses. As shown in the experimental workflow (Figure 1), samples from 4 mice in each experimental condition were collected. The whole brain was dissected into four regions, i.e., striatum, cerebellum, cortex, and "rest of the brain tissue" (ROB) that contains the substantia nigra (SN), with the purpose of identifying region-specific as well as multi-regional proteome changes. Samples from the four biological replicates per condition were pooled prior to trypsin digestion; the same amount of resulting peptides for all regions and conditions were fractionated into 25 fractions by SCX, and submitted for LC-MS/MS analysis. A total of 200 LC-MS/MS analyses were performed for all SCX fractions. After database searching against the mouse IPI protein database using the X!Tandem algorithm (23), 51,120 unique peptides were confidently identified with a false positive rate (FPR) of ~3.7% based on decoy database searching (24,28), covering 6,980 non-redundant protein groups after removing possible redundant proteins by ProteinProphet (25). 4,895 (70%) proteins with two or more unique peptides were considered to be confidently identified proteins. The proteome coverage of each brain region is summarized in Table 1. 23,894 unique peptides and 3,928 proteins were identified from the striatum region; and the other three regions have the similar trends and numbers. In addition, there are 2,945 proteins in common across all four regions. All identified peptides and proteins are listed in Supplementary Tables 1 and 2.

Spatial Protein Abundance Distribution

The spatial abundance distribution of each protein in the four analyzed brain regions was evaluated on the basis of spectral count. To illustrate the normal spatial abundance distribution, we only used data from control brain tissues for this analysis. Figure 2A shows the heatmap of ~500 proteins that are primarily localized in one or two regions among the four analyzed regions (Supplemental Table 3). Figure 2B illustrates the comparison of protein abundance patterns with mRNA abundance patterns for selected proteins. The spatial distribution patterns of protein abundances and mRNA abundances available from the Allen Brain Atlas (http://www.brain-map.org/) correlate well. Moreover, a number of these proteins are known as region-specific markers. For example, two highly-expressed proteins that were only identified in the cerebellum, cerebellin (CBLN1) and Purkinje cell protein-2 (PCP2), are associated with Purkinje cell synaptic structures (29, 30). Here we find these proteins are highly expressed in the cerebellum and absent in other brain regions (Figure 2B). CBLN1 is not shown in Figure 2B due to the lack of mRNA abundance information. Phosphodiesterase 10a (PDE10a) is highly expressed in the striatum, consistent with its known localization to striatal medium-sized spiny projection neurons and the response of these neurons to cortical stimulation (31, 32). Similarly, gamma 7 G-protein subunit (GNG7) is exclusively identified in the striatum where it is presumptively coupled to dopamine receptors (33).

NIH-PA Author Manuscript

NIH-PA Author Manuscript

NIH-PA Author Manuscript

MPTP-Induced Protein Abundance Changes

To identify region-specific protein abundance changes induced by MPTP treatment, spectral count data for each brain region were used as a semi-quantitative measurement for identifying relative abundance changes. After applying a stringent filtering criterion requiring fold-changes greater than four-fold of the standard deviation (4σ), 192, 131, 124 and 133 proteins were observed with significant abundance changes after MPTP treatment in the striatum, ROB, cortex and cerebellum, respectively, giving a total of 518 proteins with significant changes (Supplemental Table 4). 462 proteins change significantly in only one specific region after MPTP inducement. The striatum region appears to contain more proteins with significant changes than the other three regions, which is consistent with previous reports that MPTP mainly induces loss of neuron axon terminals in the striatum. Besides, region-specific protein abundance changes, we also observe a small set of proteins with consistent abundance changes across multiple brain regions with selected examples shown in Figure 3. Only one protein, plasminogen activator inhibitor 1 RNA-binding protein (Serbp1), has a consistent significant change across all four regions. A comparison of the cellular component distributions between total identified proteins and all the significantly changed proteins shows that a relatively large portion of proteins that respond to MPTP treatment are localized in mitochondria and cytoskeleton (Figure 4).

As a means to assess data quality, we were able to map our data to 41 proteins with previously reported changes in protein or gene expression associated with PD. As shown in Table 2, 37 proteins agree in the direction of the reported changes; and 12 of these proteins are known to be specifically changed in the nigrostriatal pathways due to MPTP treatment. For example, down-regulation of CSE1L, HNRPDL, COPE, ATP6V1E1 and BCAS1, and up-regulation of RAN, VIM, RPS4X, EIF4A2, UBB, THY1 and BCR were also observed in the mRNA analysis of SN from human PD subjects (34). Acetylcholinesterase precursor (ACHE) and breast carcinoma amplified sequence 1 (BCAS1), which were known to be inactivated by MPTP (35) and downregulated in SN in PD (34) were both decreased in striatum after MPTP treatment. Figure 5 further shows the fold changes of five proteins (ATPIF1, ATP6V1D, NDUFB5, NDUFS2, NDUFS7) associated with mitochondrial dysfunction that were observed with significant changes in both our previous LC-MS study in striatum using ^{18}O stable isotope labeling (22) and the present study (Figure 5A). Western blot validations on two selected proteins, ubiquitin specific protease (USP9X) and vacuolar ATP synthase subunit F (ATP6V1F), were performed and the observed changes correlate with the proteomics spectral count data (Figure 5B).

Nigrostriatal Specific Protein Abundance Changes

Proteins potentially associated with dopaminergic neurodegeneration underlying the nigrostriatal pathways can be identified by examining the patterns of protein abundance changes across the four analyzed regions. Potential nigrostriatal specific changes would occur in the striatum and/or the ROB region (containing SN) but without significant changes in the cerebellum and cortex regions. Following this data analysis, we observed a total of 270 proteins with significant nigrostriatal specific abundance changes among the 518 total regulated proteins (See Supplemental Table 5). Functional analysis of these proteins using the Ingenuity Pathways Analysis (IPA) tool (36) revealed that many of the proteins are associated with a number of functional categories, including mitochondrial dysfunction, dopamine synthesis and signaling, apoptosis, the ubiquitin system, and calcium signaling. Figure 6 shows the comparison of the number of nigrostriatal specific or total regulated proteins in each functional category. As shown, nigrostriatal specific proteins contributes to the main portion (>60%) of all functional categories, which is consistent with the knowledge that SN and striatum are the major sites of neurodegeneration in PD.

NIH-PA Author Manuscript

NIH-PA Author Manuscript

NIH-PA Author Manuscript

Functional Implications for Regulated Proteins

Table 3 lists the regulated proteins that are associated with different functional categories. The detailed protein abundance information is available in Supplementary Table 6. The abundance change patterns for each category are further displayed as heatmaps in Figure 7.

Dopamine Signaling—Of the observed 19 genes involved in dopamine signaling, 16 of them were changed significantly in MPTP treated mouse brains as shown in Figure 7A. Furthermore, fourteen of those sixteen genes with significant abundance changes were found to be specific to the striatum and the ROB regions. Protein phosphatase 1 (PPP1R14A) is the only protein which decreases significantly in the cerebellum. Serine/threonine-protein phosphatase 2a (PPP2R5E) increases significantly in both striatum and cerebellum regions. Proteins known to be associated with PD, dopa decarboxylase (DDC), tyrosine hydroxylase (TH), and monoamine oxidase B (MAOB), were detected in both the striatum and the ROB regions, which were not detected in our previous study (22). DDC is an enzyme implicated in the dopamine synthesizing metabolic pathway (37). Following the hydroxylation of tyrosine to form L-dihydroxyphenylalanine (L-DOPA) that is catalyzed by TH (38, 39), DDC decarboxylates L-DOPA to form dopamine. Both DDC and TH were found downregulated in the striatum region. MAOB, an enzyme involved in the activation of MPTP and degradation of dopamine (40, 41), was upregulated in the striatum as previously reported (42). Moreover, four other proteins in the dopamine signaling pathway (ADCY2, CLTB, RAB5A, PPP3CC) and known to be associated with neurological diseases were also observed to be down-regulated in the striatum region (43-46).

Mitochondrial Dysfunction and Oxidative Phosphorylation—58 genes associated with mitochondrial dysfunction, including subunits of each mitochondrial complex (complex I, II, III, IV and V), were detected with significant abundance changes across all four regions after MPTP treatment, suggesting that a considerable degree of mitochondrial dysfunction in the brain is induced by MPTP. Among these, changes of 32 proteins were observed in striatum and ROB regions specifically. Figure 7B shows the abundance changes for 28 selected mitochondria proteins across each complex of mitochondria dysfunction. Some of these genes were also observed with similar down-regulation in our previous study (22) (see Figure 4). In addition, a number of these genes agreed with previous mRNA expression data. For example, cytochrome c oxidase subunit VIc (COX6C), which was previously reported to be down-regulated at the mRNA level after MPTP treatment (47), was also found to be down-regulated in protein abundance in the striatum region. Moreover, ten and eleven genes were observed with significant changes only in the cerebellum or cortex region, respectively. For example, protein abundances of aldehyde dehydrogenase family 3 (ALDH3A2), fumarylacetoacetate hydrolase domain containing 1 (FAHD1), propionyl-CoA carboxylase alpha chain (PCCA) decreased significantly only in the cerebellum; while sodium/potassium-transporting ATPase (ATP1A4, ATP1B3), vacuolar ATP synthase subunit D (ATP6v0D1), and ES1 protein homolog (D10JHU81E) were down-regulated in the cortex. Five proteins with considerable abundance changes, including dodecenoyl-coenzyme A delta isomerase (DCI), nucleoside diphosphate kinase B (NME2), LAP3 protein (LAP3), glutathione S-transferase P 1 (GSTP2) and ATP synthase, H+ transporting, mitochondrial F0 complex (LOC227112), were detected not only in the striatum, but also in the cerebellum and cortex regions. LOC227112 was observed with consistent down-regulation not only in striatum and ROB, but also in the cerebellum.

Apoptosis and Cell Death—A number of proteins functionally associated with apoptosis and cell death were detected with significant abundance changes. A total of 49 proteins in this family were measured with significant changes across four regions, with 27 of them specific to the striatum or ROB regions. Some of the genes were also previously reported

NIH-PA Author Manuscript

NIH-PA Author Manuscript

NIH-PA Author Manuscript

with changes in mRNA abundances (see Supplementary Table 5). For example, the gene expression of cathepsin D precursor (CTSD) has been reported to increase Alzheimer's disease (48), and similar up-regulation was observed in our previous proteomic study (22). A number of known pro-apoptotic proteins, including clusterin (CLU), cathepsins (CTSD, CTSB), calpain small subunit 1 (CAPNS1), prolyl endopeptidase (PREP), and programmed cell death protein 8 (PDCD8), were detected with significant up-regulation in the striatum or ROB region, which is consistent with the increased loss of dopamine neurons. Anti-apoptosis proteins, astrocytic phosphoprotein PEA-15 (PEA15) and translationally-controlled tumor protein (TPT1), were observed to have significant abundance decreases following MPTP treatment. Eighteen genes changed significantly in the non-nigrostriatal regions after MPTP treatment. For example, calreticulin (CALR), programmed cell death 6-interacting protein (PDCD6IP), and protein S100-B (S100B) were up-regulated in the cerebellum or cortex. Superoxide dismutase (SOD1) and glutathione S-transferase (LOC226472) were significantly down-regulated only in the cortex region. Several antioxidant proteins, including glutathione S-transferase (GSTM5, GSTP2, LOC226472) and superoxide dismutase (SOD1), were found to be down-regulated in different regions, suggesting a decrease in anti-oxidant capacity. Moreover, we observed a significant increase in the abundance of neuronal nitric oxide synthase (nNOS in cerebellum and ROB), which could contribute to an increase in reactive nitrogen species (RNS) in the cells.

The ubiquitin system—The ubiquitin system is one of the major pathways involved in the turnover and clearance of mis-folded cellular proteins. The dysfunction of this system, such as mutations in parkin (an E3 ligase) (49) and ubiquitin carboxy-terminal hydrolase L1 (UCHL1) (50), has been causally implicated in familiar PD (51,52). A total of 149 proteins involved in the ubiquitin system were identified in this study using the KEGG PATHWAY database. Ten proteins were found with significant abundance changes in different brain regions (Table 3), and some of these changes have also been observed in other studies, for example, ubiquitin B (UBB) (34) and E3 ubiquitin-protein ligase (NEDD4) (53).

Calcium signaling—Several upregulated or downregulated proteins were observed in the calcium signaling pathway, including the downregulation of calcium/calmodulin-dependent protein kinase type IV (CAMK4), protein phosphatase 3 (PPP3CC), tropomyosin 3 (TPM3), ATP synthase (ATP5C1) in striatum. The results support the hypothesis that calcium signaling plays a role in PD.

DISCUSSION

Recent studies of PD have led to significant advances in our understanding of the pathogenesis of the disease (54-56). It has been generally recognized that the molecular mechanisms of neurodegeneration in PD involve complex interactions between environmental and genetic factors (57). Moreover, the neurodegeneration that occurs in PD extends well beyond dopaminergic neurons in the substantia nigra (SN) and striatum (7-10). In this work, we performed extensive region-specific protein abundance profiling by dividing the whole brain into four-different regions (i.e., striatum, cerebellum, cortex, and ROB), thus allowing both nigrostriatal and other region-specific proteome changes to be identified. In-depth proteome coverage was achieved by applying offline SCX fractionation coupled with capillary reversed-phase LC-MS/MS for comparative analysis of each of the brain regions from both control and MPTP treated mice.

Although the MPTP treatment leads to significant dopaminergic neuron or neuron terminal loss in SN and striatum, the effect of cell loss is corrected by using same amount of protein samples between both MPTP and control conditions for analysis. Our results revealed 518 proteins with significant abundance changes in different brain regions after MPTP treatment.

NIH-PA Author Manuscript

NIH-PA Author Manuscript

NIH-PA Author Manuscript

The majority (462 out of 518) of these proteins were observed with significant abundance changes in a single brain region, which is not surprising because each of the brain regions have very different functions. We were able to identify 270 proteins that are potentially associated with nigrostriatal pathways by observing significant abundance changes in the striatum and/or ROB, but not in the cerebellum and cortex. As anticipated, since it is known that MPTP mainly induces a loss of neuron axon terminals in the striatum, the striatum region does show more proteins that have substantial changes than the other three regions. In addition to dopaminergic neuron death, proteins observed with significant changes only in the cerebellum and cortex are of potential interest to the study other types of neurodegeneration in these regions in addition to the dopaminergic neuron death.

Functional analysis of the regulated proteins revealed a number of interesting functional categories, including mitochondrial dysfunction, dopamine synthesis and signaling, apoptosis, the ubiquitin system, and calcium signaling. This observation is consistent with recent results from both animal models and genetic models, which suggest that many of these factors that contribute significantly to PD pathogenesis (54-56). Our results revealed region-specific protein abundance changes associated with these factors. It is not surprising to observe that the majority (>60%) of proteins associated with these functional categories show nigrostriatal-specific abundance changes.

The MPTP treatment leads to ~88% decrease in dopamine levels in the striatum as measured by HPLC; therefore, one would expect a significant disruption of the dopamine synthesis and signaling pathway. However, in our previous LC-MS study (22), no proteins associated with this pathway were detected due to the sensitivity limitation of one dimensional LC-MS. In this study, we observed 16 proteins involved in the dopamine signaling pathway that exhibited significant changes after MPTP treatment. The majority of these proteins displayed changes only in the striatum and ROB regions. For example, two proteins involved in dopamine synthesis, DDC and TH, had significant decreased abundances, which are consistent with the loss of dopamine neurons.

MPTP is known to cross the blood-brain barrier and being metabolized by monoamine oxidase B (MAOB) to MPP+ in glial cells. Once converted to MPP+, it is taken up by dopaminergic neurons via the dopamine re-uptake system (dopamine transporter, DAT). MPP+ is concentrated in the mitochondria where it inhibits the complex I of the respiratory chain, leading to ATP depletion and increased generation of reactive oxygen species (ROS) such as superoxide anion and hydroxyl radical, leading to the cell death of dopaminergic neurons (55,58). Mitochondrial dysfunction indeed contributes to a wide range of human pathologies, including multiple neurodegenerative diseases, ischaemia-reperfusion injury in stroke and heart attack, diabetes and the cumulative degeneration associated with aging. It causes cell damage and death by compromising ATP production, disrupting calcium homeostasis and increasing oxidative stress. Furthermore, mitochondrial damage can lead to apoptotic cell death by causing the release of cytochrome c and other pro-apoptotic factors into the cytoplasm (55). Consistent with our previous observation of protein abundance changes associated with mitochondrial dysfunction (22), the current study considerably expanded the coverage of proteins associated with this function. In total we observed ~58 proteins with significant abundance changes that cover all five subunits of each complex (complexes I, II, III, IV and V). Our data further consolidates the pivotal function of mitochondria in PD neurodegeneration. Some proteins associated with oxidative stress response were also observed with significant abundance changes, which include glutathione S-transferase MU 5 (GSTM5), endoplasmic reticulum protein (ERP29), carbonyl reductase 1 (CBR1), cullin-3 (CUL3) and neuronal growth regulator 1 (NEGR1).

NIH-PA Author Manuscript

NIH-PA Author Manuscript

NIH-PA Author Manuscript

In addition to mitochondrial dysfunction and oxidative stress, we also identified numerous proteins functionally associated with apoptosis and cell death. Mitochondria are known to be pivotal in controlling apoptosis since they house many apoptogenic molecules that are released into the cytoplasm at the onset of apoptosis (55). These include cytochrome c, apoptosis-inducing factor and various caspases. In general, we observed up-regulation for pro-apoptotic proteins, and down-regulation for anti-apoptotic proteins, supportive of the increased cell death caused by MPTP. The increased apoptosis due to MPTP induction is also reflected by the decreased anti-oxidant capacity shown by the down-regulation of a number of known antioxidant proteins and the increased expression of neuronal nitric oxide synthase.

Our data also provide several lines of evidence that MPTP induced neurodegeneration may not be limited to the nigrostriatal regions. First, significant changes for a number of proteins associated with apoptosis and antioxidant functions were observed specifically in the cortex and cerebellum. For example, calreticulin (CALR), nitric-oxide synthase (NOS1) and programmed cell death 6-interacting protein (PDCD6IP), protein S100-B (S100B) were up-regulated in the cerebellum or cortex only. Similarly, a number of proteins associated with mitochondria dysfunction such as NADH dehydrogenase 1 (NDUFA9), NADH-ubiquinone oxidoreductase (NDUFS2, NDUFV1), sodium/potassium-transporting ATPase (ATP1a4, ATP1b3), beta-synuclein (SNCB) were also observed to have significant changes only in the cortex or cerebellum. As the cerebellum does not contain dopaminergic neurons, the observed effects of MPTP might derive from the glial cells or be related from other regions of the brain.

Several proteins from the ubiquitin system were observed with significant abundance changes in different brain regions. One interesting protein is ubiquitin-specific protease USP9X (2559 amino acid) that has a completely different sequence from a known Parkinson's disease gene, UCHL1 (223 amino acid) (50). USP9X was significantly upregulated in the striatum, cerebellum and cortex with Western blot validations (Figure 6). USP9X, also known as FAM, is a mammalian homolog of Drosophila fat facets (59), which is an enzyme required for eye development and early embryogenesis (60,61). USP9X deubiquitination prevents the proteasomal degradation of some substrates such as Af-6 (62) and beta-catenin (63), but also regulates the activity and intracellular localization of other substrates, such as epsin (64) and MARCH 7 (65). Therefore, a possible way for USP9X to be involved in PD is that during the development of PD, USP9X affects the degradation of alpha synuclein, leading to toxic aggregation. A recent study (66) reported that USP9X activates SMAD4 by deubiquitination at K519, resulting in the activation of SMAD2/3, and promotion of TGFβ pathway, which will induce cell apoptosis (67). The involvement of USP9X in apoptosis is confirmed by the data from the homolog fat facets, which is an enhancer of grim-reaper induced apoptosis in Drosophila (68). Considering that TGFb1 (69) and TGFb2 (70) were associated with neurodegenerative diseases, USP9X is possibly a novel protein involved in the development of PD by both promoting the TGFβ pathway and inducing the apoptosis of cells. In addition, USP9X is reported to interact with Huntingtin protein (71) raising the possibility of a general role for USP9X in neurodegeneration.

Calcium signaling is known to regulate multiple neuronal functions, including synaptic transmission, plasticity, and cell survival (72). High cytosolic Ca^{2+} can induce oxidative stress and excitotoxicity and has long been suspected to play a role in PD (73,74). Recent evidence indicates that neuronal calcium signaling is abnormal in many neurodegenerative disorders, including AD and PD (75). Elevated intracellular Ca^{2+} participates in SN cell loss (76). Our observation of abundance changes in proteins associated with calcium signaling provides further evidence of its potential role in PD.

NIH-PA Author Manuscript

NIH-PA Author Manuscript

NIH-PA Author Manuscript

To summarize, our extensive proteome survey provides a comprehensive picture of protein abundance changes in different brain regions induced by MPTP treatment, the most commonly used mouse model for PD. The observed protein abundance changes are also supportive of the general mechanism of MPTP induced neurodegeneration as shown in Figure 8. Briefly, MPP+ induces mitochondria dysfunction, which leads to a decreased antioxidant capacity and the generation of excessive ROS and RNS. The oxidative stress condition leads to an up-regulation of pro-apoptotic proteins or factors, down-regulation of anti-apoptotic proteins, and disruption of the ubiquitin system, all of which eventually lead to cell death. Although our data supports that neurodegeneration mainly occurs in the nigrostriatal region, the study does provide additional novel information potentially associated with the neurodegeneration outside this region. It is not clear that all changes observed are associated with neurodegeneration. It may well be that some changes in protein expression represent the brain's attempts to rectify trauma or detoxify the cells. We believe this dataset contains a rich source of novel proteins, e.g., USP9X, that may play an important role in neurological diseases and many of the proteins may represent interesting targets for further hypothesis-driven mechanistic studies.

Supplementary Material

Refer to Web version on PubMed Central for supplementary material.

Acknowledgments

Portions of this research were supported by the NIH Center of Proteomics Research Resource for Integrative Biology RR018522 (to R.D.S.), NIH grants R01 NS050148 (to D.J.S.) and the Pacific Northwest National Laboratory (PNNL) Directed Research Development program (to W.J.Q.). The experiment work was performed in the Environmental Molecular Sciences Laboratory, a U.S. Department of Energy (DOE) national scientific user facility on the PNNL campus. PNNL is multi-program national laboratory operated by Battelle for the DOE under Contract No. DE-AC05-76RLO 1830.

Abbreviations

(PD)	Parkinson's disease
(SN)	Substantia nigra
(MPTP)	1-Methyl-4-phenyl-1, 2, 3, 6-tetrahydropyridine
(2DE)	Two-dimensional electrophoresis
(IPI)	International Protein Index
(SCX)	Strong cation exchange
(SPE)	Solid phase extraction
(TFE)	Trifluoroethanol
(TBP)	Tributylphosphine
(ROS)	Radical oxygen species
(RNS)	Radical nitrogen species
(MPP)	1-Methyl-4-phenylpyridinium
(DAT)	Dopamine transporter
(ATP)	Adenosine-5′-triphosphate

NIH-PA Author Manuscript

NIH-PA Author Manuscript

NIH-PA Author Manuscript

REFERENCES

1. Jenner P, Olanow CW. Understanding cell death in Parkinson's disease. Ann Neurol 1998;44:S72–84. [PubMed: 9749577]
2. Olanow CW, Tatton WG. Etiology and pathogenesis of Parkinson's disease. Annu Rev Neurosci 1999;22:123–144. [PubMed: 10202534]
3. Forno LS, DeLanney LE, Irwin I, Langston JW. Electron microscopy of Lewy bodies in the amygdala-parahippocampal region. Comparison with inclusion bodies in the MPTP-treated squirrel monkey. Adv Neurol 1996;69:217–228. [PubMed: 8615131]
4. Parkinson J. an essay on the shaking palsy. J. Neuropsychiatry Clin. Neurosci 1817:223–236.
5. Dawson TM, Dawson VL. Molecular pathways of neurodegeneration in Parkinson's disease. Science 2003;302:819–822. [PubMed: 14593166]
6. Belin AC, Westerlund M. Parkinson's disease: a genetic perspective. FEBS J 2008;275:1377–1383. [PubMed: 18279377]
7. Dauer W, Przedborski S. Parkinson's disease: mechanisms and models. Neuron 2003;39:889–909. [PubMed: 12971891]
8. Przedborski S, Vila M. The 1-methyl-4-phenyl-1,2,3,6-tetrahydropyridine mouse model: a tool to explore the pathogenesis of Parkinson's disease. Ann N Y Acad Sci 2003;991:189–198. [PubMed: 12846987]
9. Forno LS, DeLanney LE, Irwin I, Langston JW. Similarities and differences between MPTP-induced parkinsonsim and Parkinson's disease. Neuropathologic considerations. Adv Neurol 1993;60:600–608. [PubMed: 8380528]
10. Heikkila RE, Hess A, Duvoisin RC. Dopaminergic neurotoxicity of 1-methyl-4-phenyl-1,2,5,6-tetrahydropyridine in mice. Science 1984;224:1451–1453. [PubMed: 6610213]
11. Javitch JA, D'Amato RJ, Strittmatter SM, Snyder SH. Parkinsonism-inducing neurotoxin, N-methyl-4-phenyl-1,2,3,6 -tetrahydropyridine: uptake of the metabolite N-methyl-4-phenylpyridine by dopamine neurons explains selective toxicity. Proc Natl Acad Sci U S A 1985;82:2173–2177. [PubMed: 3872460]
12. Burns RS, Chiueh CC, Markey SP, Ebert MH, Jacobowitz DM, Kopin IJ. A primate model of parkinsonism: selective destruction of dopaminergic neurons in the pars compacta of the substantia nigra by N-methyl-4-phenyl-1,2,3,6-tetrahydropyridine. Proc Natl Acad Sci USA 1983;80:4546–4550. [PubMed: 6192438]
13. Hornykiewicz O, Kish SJ. Biochemical pathophysiology of Parkinson's disease. Adv Neurol 1987;45:19–34. [PubMed: 2881444]
14. Fountoulakis M, Kossida S. Proteomics-driven progress in neurodegeneration research. Electrophoresis 2006;27:1556–1573. [PubMed: 16555340]
15. Zhang J, Goodlett DR. Proteomic approach to studying Parkinson's disease. Mol. Neurobiol 2004;29:271–288. [PubMed: 15181239]
16. Periquet M, Corti O, Jacquier S, Brice A. Proteomic analysis of parkin knockout mice: alterations in energy metabolism, protein handling and synaptic function. J Neurochem 2005;95:1259–1276. [PubMed: 16150055]
17. Palacino JJ, Sagi D, Goldberg MS, Krauss S, Motz C, Wacker M, Klose J, Shen J. Mitochondrial dysfunction and oxidative damage in parkin-deficient mice. J Biol Chem 2004;279:18614–18622. [PubMed: 14985362]
18. Basso M, Giraudo S, Corpillo D, Bergamasco B, Lopiano L, Fasano M. Proteome analysis of human substantia nigra in Parkinson's disease. Proteomics 2004;4:3943–3952. [PubMed: 15526345]
19. Jin J, Hulette C, Wang Y, Zhang T, Pan C, Wadhwa R, Zhang J. Proteomic identification of a stress protein, mortalin/mthsp70/GRP75: relevance to Parkinson disease. Mol Cell Proteomics 2006;5:1193–1204. [PubMed: 16565515]
20. Jin J, Meredith GE, Chen L, Zhou Y, Xu J, Shie FS, Lockhart P, Zhang J. Quantitative proteomic analysis of mitochondrial proteins: relevance to Lewy body formation and Parkinson's disease. Brain Res Mol Brain Res 2005;134:119–138. [PubMed: 15790536]

NIH-PA Author Manuscript

NIH-PA Author Manuscript

NIH-PA Author Manuscript

21. Diedrich M, Mao L, Bernreuther C, Zabel C, Nebrich G, Kleene R, Klose J. Proteome analysis of ventral midbrain in MPTP-treated normal and L1cam transgenic mice. Proteomics 2008;8:1266–1275. [PubMed: 18338827]
22. Chin MH, Qian WJ, Wang H, Petyuk VA, Bloom JS, Sforza DM, Lacan G, Liu D, Khan AH, Cantor RM, Bigelow DJ, Melega WP, Camp DG 2nd, Smith RD, Smith DJ. Mitochondrial dysfunction, oxidative stress, and apoptosis revealed by proteomic and transcriptomic analyses of the striata in two mouse models of Parkinson's disease. J Proteome Res 2008;7:666–677. [PubMed: 18173235]
23. Fenyo D, Beavis RC. A method for assessing the statistical significance of mass spectrometry-based protein identifications using general scoring schemes. Anal Chem 2003;75:768–774. [PubMed: 12622365]
24. Qian WJ, Liu T, Monroe ME, Strittmatter EF, Jacobs JM, Kangas LJ, Petritis K, Camp DG 2nd, Smith RD. Probability-based evaluation of peptide and protein identifications from tandem mass spectrometry and SEQUEST analysis: the human proteome. J Proteome Res 2005;4:53–62. [PubMed: 15707357]
25. Nesvizhskii AI, Keller A, Kolker E, Aebersold R. A statistical model for identifying proteins by tandem mass spectrometry. Anal Chem 2003;75:4646–4658. [PubMed: 14632076]
26. Qian WJ, Jacobs JM, Camp DG 2nd, Monroe ME, Moore RJ, Gritsenko MA, Calvano SE, Lowry SF, Xiao W, Moldawer LL, Davis RW, Tompkins RG, Smith RD. Comparative proteome analyses of human plasma following in vivo lipopolysaccharide administration using multidimensional separations coupled with tandem mass spectrometry. Proteomics 2005;5:572–584. [PubMed: 15627965]
27. Kanai-Azuma M, Mattick JS, Kaibuchi K, Wood SA. Co-localization of FAM and AF-6, the mammalian homologues of Drosophila faf and canoe, in mouse eye development. Mech Dev 2000;91:383–386. [PubMed: 10704870]
28. Elias JE, Gygi SP. Target-decoy search strategy for increased confidence in large-scale protein identifications by mass spectrometry. Nat Methods 2007;4:207–214. [PubMed: 17327847]
29. Urade Y, Oberdick J, Molinar-Rode R, Morgan JI. Precerebellin is a cerebellum-specific protein with similarity to the globular domain of complement C1q B chain. Proc Natl Acad Sci USA 1991;88:1069–1073. [PubMed: 1704129]
30. Guan J, Luo Y, Denker BM. Purkinje cell protein-2 (Pcp2) stimulates differentiation in PC12 cells by Gbetagamma-mediated activation of Ras and p38 MAPK. Biochem J 2005;392:389–397. [PubMed: 15948714]
31. Fujishige K, Kotera J, Omori K. Striatum- and testis-specific phosphodiesterase PDE10A isolation and characterization of a rat PDE10A. Eur J Biochem 1999;266:1118–1127. [PubMed: 10583409]
32. Threlfell S, Sammut S, Menniti FS, Schmidt CJ, West AR. Inhibition of Phosphodiesterase 10A Increases the Responsiveness of Striatal Projection Neurons to Cortical Stimulation. J Pharmacol Exp Ther 2009;328:785–795. [PubMed: 19056933]
33. Danielson PE, Watson JB, Gerendasy DD, Erlander MG, Lovenberg TW, de Lecea L, Sutcliffe JG, Frankel WN. Chromosomal mapping of mouse genes expressed selectively within the central nervous system. Genomics 1994;19:454–461. [PubMed: 7910582]
34. Kim JM, Lee KH, Jeon YJ, Oh JH, Jeong SY, Song IS, Lee DS, Kim NS. Identification of genes related to Parkinson's disease using expressed sequence tags. DNA Res 2006;13:275–286. [PubMed: 17213182]
35. Zang LY, Misra HP. Inactivation of acetylcholinesterase by 1-methyl-4-phenyl-1,2,3,6-tetrahydropyridine hydrochloride. Mol Cell Biochem 2003;254:131–136. [PubMed: 14674691]
36. Calvano SE, Xiao W, Richards DR, Felciano RM, Baker HV, Cho RJ, Chen RO, Brownstein BH, Cobb JP, Tschoeke SK, Miller-Graziano C, Moldawer LL, Mindrinos MN, Davis RW, Tompkins RG, Lowry SF. A network-based analysis of systemic inflammation in humans. Nature 2005;437:1032–1037. [PubMed: 16136080]
37. Burkhard P, Dominici P, Borri-Voltattorni C, Jansonius JN, Malashkevich VN. Structural insight into Parkinson's disease treatment from drug-inhibited DOPA decarboxylase. Nat Struct Biol 2001;8:963–967. [PubMed: 11685243]

NIH-PA Author Manuscript

NIH-PA Author Manuscript

NIH-PA Author Manuscript

38. Jackson-Lewis V, Jakowec M, Burke RE, Przedborski S. Time course and morphology of dopaminergic neuronal death caused by the neurotoxin 1-methyl-4-phenyl-1,2,3,6-tetrahydropyridine. Neurodegeneration 1995;4:257–269. [PubMed: 8581558]
39. Tatton WG, Kwan MM, Verrier MC, Seniuk NA, Theriault E. MPTP produces reversible disappearance of tyrosine hydroxylase-containing retinal amacrine cells. Brain Res 1990;527:21–31. [PubMed: 1980839]
40. Heikkila RE, Manzino L, Cabbat FS, Duvoisin RC. Protection against the dopaminergic neurotoxicity of 1-methyl-4-phenyl-1,2,5,6-tetrahydropyridine by monoamine oxidase inhibitors. Nature 1984;311:467–469. [PubMed: 6332989]
41. Trevor AJ, Singer TP, Ramsay RR, Castagnoli N Jr. Processing of MPTP by monoamine oxidases: implications for molecular toxicology. J Neural Transm Suppl 1987;23:73–89. [PubMed: 3295117]
42. Damier P, Kastner A, Agid Y, Hirsch EC. Does monoamine oxidase type B play a role in dopaminergic nerve cell death in Parkinson's disease? Neurology 1996;46:1262–1269. [PubMed: 8628464]
43. Laifenfeld D, Patzek LJ, McPhie DL, Chen Y, Levites Y, Cataldo AM, Neve RL. Rab5 mediates an amyloid precursor protein signaling pathway that leads to apoptosis. J Neurosci 2007;27:7141–7153. [PubMed: 17611268]
44. Li H, Wetten S, Li L, St Jean PL, Upmanyu R, Surh L, Hosford D, Barnes MR, Briley JD, Borrie M, Coletta N, Delisle R, Dhalla D, Ehm MG, Feldman HH, Fornazzari L, Gauthier S, Goodgame N, Guzman D, Hammond S, Hollingworth P, Hsiung GY, Johnson J, Kelly DD, Keren R, Kertesz A, King KS, Lovestone S, Loy-English I, Matthews PM, Owen MJ, Plumpton M, Pryse-Phillips W, Prinjha RK, Richardson JC, Saunders A, Slater AJ, St George-Hyslop PH, Stinnett SW, Swartz JE, Taylor RL, Wherrett J, Williams J, Yarnall DP, Gibson RA, Irizarry MC, Middleton LT, Roses AD. Candidate single-nucleotide polymorphisms from a genomewide association study of Alzheimer disease. Arch Neurol 2008;65:45–53. [PubMed: 17998437]
45. Hakak Y, Walker JR, Li C, Wong WH, Davis KL, Buxbaum JD, Haroutunian V, Fienberg AA. Genome-wide expression analysis reveals dysregulation of myelination-related genes in chronic schizophrenia. Proc Natl Acad Sci USA 2001;98:4746–4751. [PubMed: 11296301]
46. Carter CJ. eIF2B and oligodendrocyte survival: where nature and nurture meet in bipolar disorder and schizophrenia? Schizophr Bull 2007;33:1343–1353. [PubMed: 17329232]
47. Gomez-Gallego M, Fernandez-Villalba E, Fernandez-Barreiro A, Herrero MT. Changes in the neuronal activity in the pedunculopontine nucleus in chronic MPTP-treated primates: an in situ hybridization study of cytochrome oxidase subunit I, choline acetyl transferase and substance P mRNA expression. J Neural Transm 2007;114:319–326. [PubMed: 16988796]
48. Yan S, Sloane BF. Molecular regulation of human cathepsin B: implication in pathologies. Biol Chem 2003;384:845–854. [PubMed: 12887051]
49. Shimura H, Hattori N, Kubo S, Mizuno Y, Asakawa S, Minoshima S, Shimizu N, Iwai K, Chiba T, Tanaka K, Suzuki T. Familial Parkinson disease gene product, parkin, is a ubiquitin-protein ligase. Nat Genet 2000;25:302–305. [PubMed: 10888878]
50. Leroy E, Boyer R, Auburger G, Leube B, Ulm G, Mezey E, Harta G, Brownstein MJ, Jonnalagada S, Chernova T, Dehejia A, Lavedan C, Gasser T, Steinbach PJ, Wilkinson KD, Polymeropoulos MH. The ubiquitin pathway in Parkinson's disease. Nature 1998;395:451–452. [PubMed: 9774100]
51. Giasson BI, Lee VM. Are ubiquitination pathways central to Parkinson's disease? Cell 2003;114:1–8. [PubMed: 12859888]
52. Rubinsztein DC. The roles of intracellular protein-degradation pathways in neurodegeneration. Nature 2006;443:780–786. [PubMed: 17051204]
53. Dil Kuazi A, Kito K, Abe Y, Shin RW, Kamitani T, Ueda N. NEDD8 protein is involved in ubiquitinated inclusion bodies. J Pathol 2003;199:259–266. [PubMed: 12533840]
54. Eriksen JL, Wszolek Z, Petrucelli L. Molecular pathogenesis of Parkinson disease. Arch Neurol 2005;62:353–357. [PubMed: 15767499]
55. Lin MT, Beal MF. Mitochondrial dysfunction and oxidative stress in neurodegenerative diseases. Nature 2006;443:787–795. [PubMed: 17051205]

NIH-PA Author Manuscript

NIH-PA Author Manuscript

NIH-PA Author Manuscript

56. Olanow CW. The pathogenesis of cell death in Parkinson's disease - 2007. Mov Disord 2007;22:S335–S342. [PubMed: 18175394]
57. Maraganore DM, de Andrade M, Lesnick TG, Farrer MJ, Bower JH, Hardy JA, Rocca WA. Complex interactions in Parkinson's disease: a two-phased approach. Mov Disord 2003;18:631–636. [PubMed: 12784265]
58. Hasegawa E, Takeshige K, Oishi T, Murai Y, Minakami S. 1-Methyl-4-phenylpyridinium (MPP+) induces NADH-dependent superoxide formation and enhances NADH-dependent lipid peroxidation in bovine heart submitochondrial particles. Biochem Biophys Res Commun 1990;170:1049–1055. [PubMed: 2167668]
59. Wood SA, Pascoe WS, Ru K, Yamada T, Hirchenhain J, Kemler R, Mattick JS. Cloning and expression analysis of a novel mouse gene with sequence similarity to the Drosophila fat facets gene. Mech Dev 1997;63:29–38. [PubMed: 9178254]
60. Chen X, Overstreet E, Wood SA, Fischer JA. On the conservation of function of the Drosophila fat facets deubiquitinating enzyme and Fam, its mouse homolog. Dev Genes Evol 2000;210:603–610. [PubMed: 11151297]
61. Pantaleon M, Kanai-Azuma M, Mattick JS, Kaibuchi K, Kaye PL, Wood SA. FAM deubiquitylating enzyme is essential for preimplantation mouse embryo development. Mech Dev 2001;109:151–160. [PubMed: 11731229]
62. Taya S, Yamamoto T, Kano K, Kawano Y, Iwamatsu A, Tsuchiya T, Tanaka K, Kanai-Azuma M, Wood SA, Mattick JS, Kaibuchi K. The Ras target AF-6 is a substrate of the fam deubiquitinating enzyme. J Cell Biol 1998;142:1053–1062. [PubMed: 9722616]
63. Taya S, Yamamoto T, Kanai-Azuma M, Wood SA, Kaibuchi K. The deubiquitinating enzyme Fam interacts with and stabilizes beta-catenin. Genes Cells 1999;4:757–767. [PubMed: 10620020]
64. Chen H, Polo S, Di Fiore PP, De Camilli PV. Rapid Ca2+-dependent decrease of protein ubiquitination at synapses. Proc Natl Acad Sci USA 2003;100:14908–14913. [PubMed: 14657369]
65. Nathan JA, Sengupta S, Wood SA, Admon A, Markson G, Sanderson C, Lehner PJ. The ubiquitin E3 ligase MARCH7 is differentially regulated by the deubiquitylating enzymes USP7 and USP9X. Traffic 2008;9:1130–1145. [PubMed: 18410486]
66. Dupont S, Mamidi A, Cordenonsi M, Montagner M, Zacchigna L, Adorno M, Martello G, Stinchfield MJ, Soligo S, Morsut L, Inui M, Moro S, Modena N, Argenton F, Newfeld SJ, Piccolo S. FAM/USP9x, a deubiquitinating enzyme essential for TGFbeta signaling, controls Smad4 monoubiquitination. Cell 2009;136:123–135. [PubMed: 19135894]
67. Valderrama-Carvajal H, Cocolakis E, Lacerte A, Lee EH, Krystal G, Ali S, Lebrun JJ. Activin/TGF-beta induce apoptosis through Smad-dependent expression of the lipid phosphatase SHIP. Nat Cell Biol 2002;4:963–969. [PubMed: 12447389]
68. Wing JP, Schreader BA, Yokokura T, Wang Y, Andrews PS, Huseinovic N, Dong CK, Ogdahl JL, Schwartz LM, White K, Nambu JR. Drosophila Morgue is an F box/ubiquitin conjugase domain protein important for grim-reaper mediated apoptosis. Nat Cell Biol 2002;4:451–456. [PubMed: 12021772]
69. Rota E, Bellone G, Rocca P, Bergamasco B, Emanuelli G, Ferrero P. Increased intrathecal TGF-beta1, but not IL-12, IFN-gamma and IL-10 levels in Alzheimer's disease patients. Neurol Sci 2006;27:33–39. [PubMed: 16688597]
70. Goris A, Williams-Gray CH, Foltynie T, Brown J, Maranian M, Walton A, Compston DA, Barker RA, Sawcer SJ. Investigation of TGFB2 as a candidate gene in multiple sclerosis and Parkinson's disease. J Neurol 2007;254:846–848. [PubMed: 17431704]
71. Kaltenbach LS, Romero E, Becklin RR, Chettier R, Bell R, Phansalkar A, Strand A, Torcassi C, Savage J, Hurlburt A, Cha GH, Ukani L, Chepanoske CL, Zhen Y, Sahasrabudhe S, Olson J, Kurschner C, Ellerby LM, Peltier JM, Botas J, Hughes RE. Huntingtin interacting proteins are genetic modifiers of neurodegeneration. PLoS Genet 2007;3:e82. [PubMed: 17500595]
72. Wojda U, Salinska E, Kuznicki J. Calcium ions in neuronal degeneration. IUBMB Life 2008;60(9):575–90. [PubMed: 18478527]
73. Beal MF. Excitotoxicity and nitric oxide in Parkinson's disease pathogenesis. Annals of neurology 1998;44:S110–114. [PubMed: 9749581]

NIH-PA Author Manuscript

NIH-PA Author Manuscript

NIH-PA Author Manuscript

74. Chan CS, Guzman JN, Ilijic E, Mercer JN, Rick C, Tkatch T, Meredith GE, Surmeier DJ. 'Rejuvenation' protects neurons in mouse models of Parkinson's disease. Nature 2007;447:1081–1086. [PubMed: 17558391]

75. Bezprozvanny I. Calcium signaling and neurodegenerative diseases. Trends Mol Med 2009;15:89–100. [PubMed: 19230774]

76. Sulzer D, Schmitz Y. Parkinson's disease: return of an old prime suspect. Neuron 2007;55:8–10. [PubMed: 17610813]

77. Zhang Y, Dawson VL, Dawson TM. Oxidative stress and genetics in the pathogenesis of Parkinson's disease. Neurobiology of disease 2000;7:240–250. [PubMed: 10964596]

78. Gorman AM, Ceccatelli S, Orrenius S. Role of mitochondria in neuronal apoptosis. Dev Neurosci 2000;22:348–358. [PubMed: 11111150]

79. Mollenhauer B, Steinacker P, Bahn E, Bibl M, Brechlin P, Schlossmacher MG, Locascio JJ, Wiltfang J, Kretzschmar HA, Poser S, Trenkwalder C, Otto M. Serum heart-type fatty acid-binding protein and cerebrospinal fluid tau: marker candidates for dementia with Lewy bodies. Neurodegener Dis 2007;4:366–375. [PubMed: 17622779]

80. Galter D, Buervenich S, Carmine A, Anvret M, Olson L. ALDH1 mRNA: presence in human dopamine neurons and decreases in substantia nigra in Parkinson's disease and in the ventral tegmental area in schizophrenia. Neurobiology of disease 2003;14:637–647. [PubMed: 14678778]

81. Culvenor JG, McLean CA, Cutt S, Campbell BC, Maher F, Jakala P, Hartmann T, Beyreuther K, Masters CL, Li QX. Non-Abeta component of Alzheimer's disease amyloid (NAC) revisited. NAC and alpha-synuclein are not associated with Abeta amyloid. Am J Pathol 1999;155:1173–1181. [PubMed: 10514400]

82. Fan Y, Limprasert P, Murray IV, Smith AC, Lee VM, Trojanowski JQ, Sopher BL, La Spada AR. Beta-synuclein modulates alpha-synuclein neurotoxicity by reducing alpha-synuclein protein expression. Human molecular genetics 2006;15:3002–3011. [PubMed: 16959793]

83. Dev KK, van der Putten H, Sommer B, Rovelli G. Part I: parkin-associated proteins and Parkinson's disease. Neuropharmacology 2003;45:1–13. [PubMed: 12814656]

84. Ko HS, Kim SW, Sriram SR, Dawson VL, Dawson TM. Identification of far upstream element-binding protein-1 as an authentic Parkin substrate. The Journal of biological chemistry 2006;281:16193–16196. [PubMed: 16672220]

85. Chassain C, Bielicki G, Durand E, Lolignier S, Essafi F, Traore A, Durif F. Metabolic changes detected by proton magnetic resonance spectroscopy in vivo and in vitro in a murin model of Parkinson's disease, the MPTP-intoxicated mouse. Journal of neurochemistry 2008;105:874–882. [PubMed: 18088356]

86. Buchwald P, Juhasz A, Bell C, Patfalusi M, Kovacs P, Hochhaus G, Howes J, Bodor N. Influence of the N-acetylation polymorphism on the metabolism of talampanel: an investigation in fasted and fed subjects genotyped for NAT2 variants. Pharmazie 2006;61:125–134. [PubMed: 16526560]

NIH-PA Author Manuscript

NIH-PA Author Manuscript

NIH-PA Author Manuscript

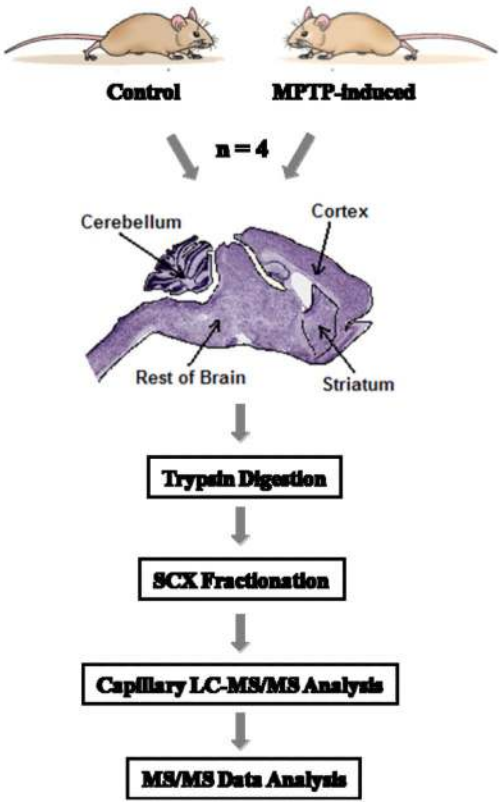

Figure 1.
Flowchart showing the experimental workflow.

NIH-PA Author Manuscript

NIH-PA Author Manuscript

NIH-PA Author Manuscript

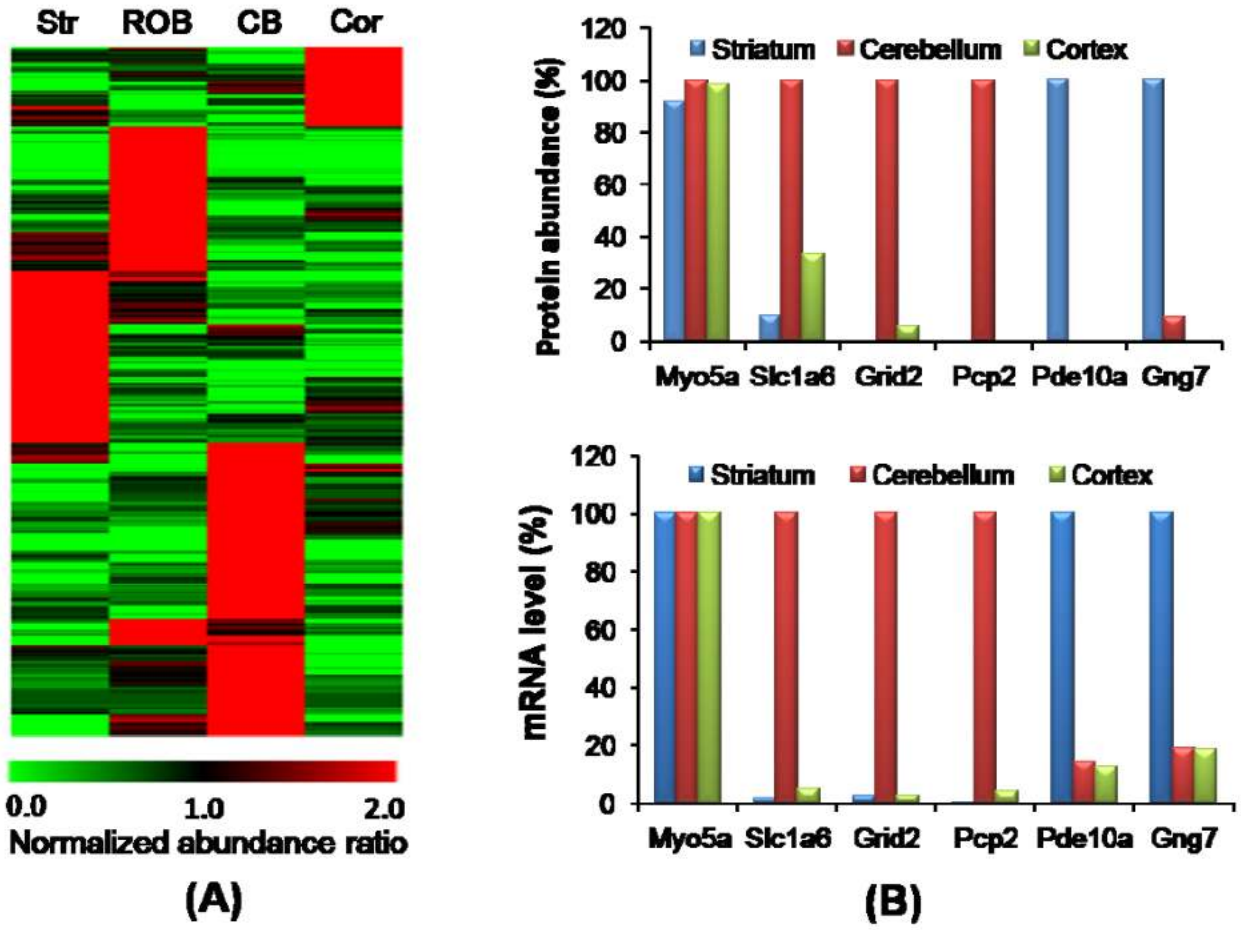

Figure 2.

(A) Heatmap of ~500 region-specific proteins from control brain samples. Protein abundances were displayed with a normalized abundance ratio scale where the spectral count for each protein in a given region was divided by the average spectral count across the four regions. All proteins had at least five total spectral counts and the normalized abundance ratio was >3 in at least one region. (Str: striatum; ROB: rest of brain; CB: cerebellum; Cor: Cortex) (B) Selected localized proteins showing good agreement with mRNA abundance distributions available in the Allen Brain Atlas (http://www.brain-map.org/). The ROB is not included because the average data for the rest of brain region is less quantitative. The highest region abundance of each protein is set as 100%. Myosin-5A (MYO5A) is a general protein expressed the same across all brain regions.

NIH-PA Author Manuscript

NIH-PA Author Manuscript

NIH-PA Author Manuscript

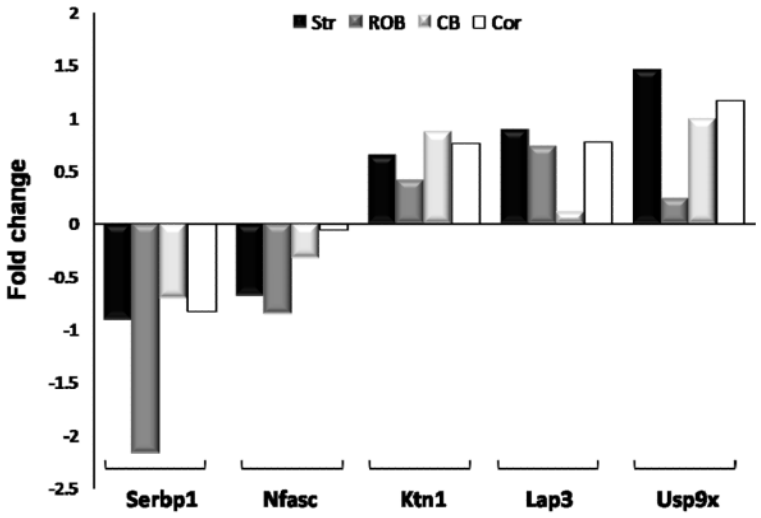

Figure 3.
MPTP induced protein abundance changes for selected proteins across the four regions. Abundance changes were displayed as fold changes where the fold change is [MPTP]/[Ctrl]-1 if abundance ratio of spectral count ≥1, or the fold change is 1-[Ctrl]/[MPTP] if abundance ratio <1. Region annotations: Str: striatum; ROB: rest of brain; CB: cerebellum; Cor: Cortex.

NIH-PA Author Manuscript

NIH-PA Author Manuscript

NIH-PA Author Manuscript

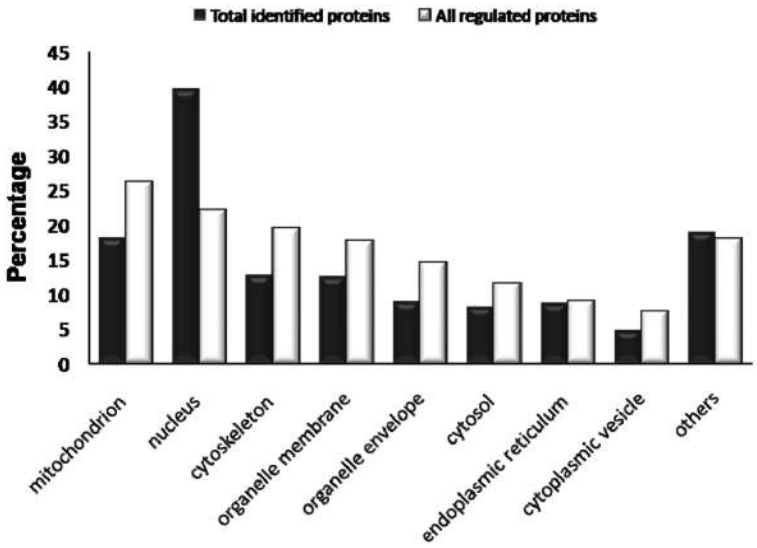

Figure 4.

Comparison of the cellular component distributions between the total identified proteins (black) and all regulated proteins (white) that show significant MPTP-induced abundance changes. The number of proteins in each category is expressed as a percentage of the total.

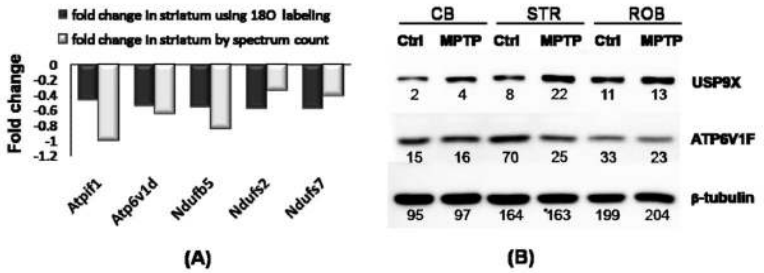

Figure 5.

(A) Fold changes observed for selected mitochondrial proteins in the striatum. Fold-changes from ^{18}O labeling is detailed in a previous paper[22]. (B) Western blot analysis of ubiquitin carboxyl-terminal hydrolase (USP9X) and vacuolar ATP synthase subunit F (ATP6v1f) in three different mouse brain regions before and after MPTP treatment. The spectral count for a protein in each brain region is labeled under each gel band. USP9X is observed to be up-regulated in all three regions. ATP6v1f is observed to be down-regulated in STR and ROB regions with MPTP treatment. The results agree with the proteome data. (STR: striatum; CB: cerebellum)

NIH-PA Author Manuscript NIH-PA Author Manuscript NIH-PA Author Manuscript

NIH-PA Author Manuscript

NIH-PA Author Manuscript

NIH-PA Author Manuscript

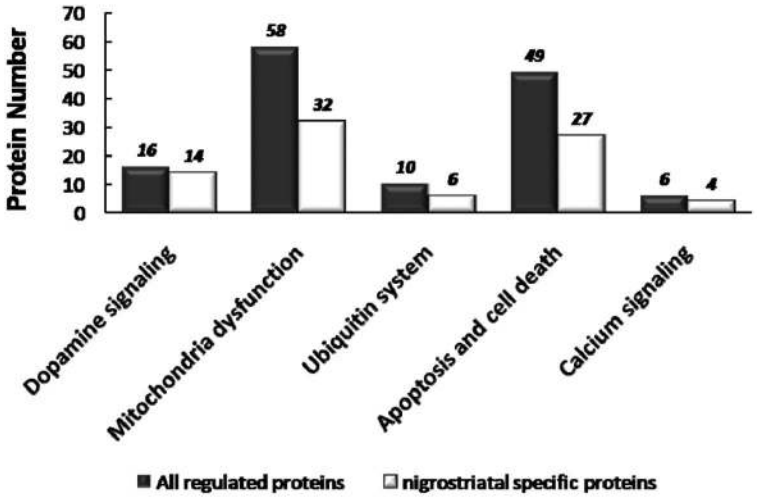

Figure 6.
Comparison of the number of nigrostriatal-specific and total significant proteins in each functional category. Nigrostriatal-specific proteins contribute to the main portion (>60%) of all functional categories.

NIH-PA Author Manuscript

NIH-PA Author Manuscript

NIH-PA Author Manuscript

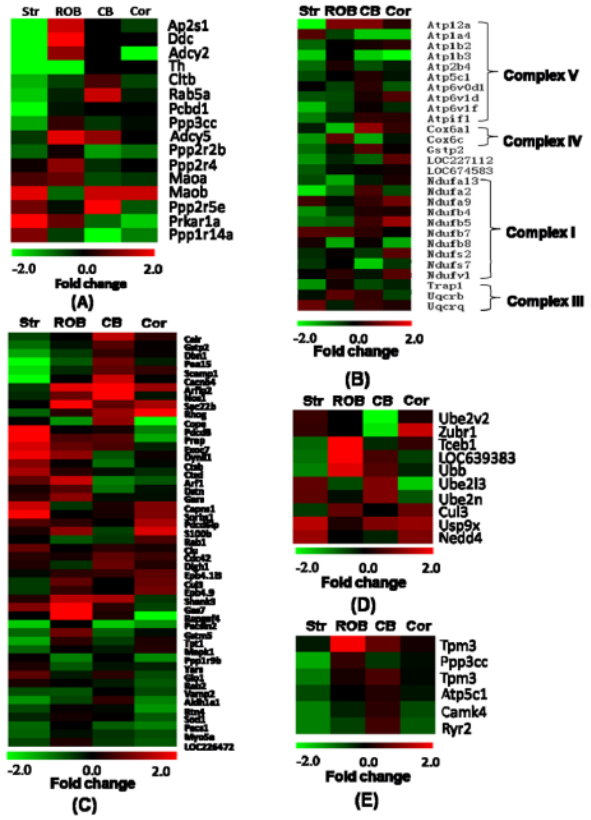

Figure 7.

Heat maps of abundance changes for specific protein functional categories. (A) Dopamine signaling pathway; (B) Mitochondrial dysfunction; (C) Apoptosis and cell death; (D) the ubiquitin system; (E) Calcium signaling. Relative protein abundances are displayed as fold changes (MPTP/control).

NIH-PA Author Manuscript

NIH-PA Author Manuscript

NIH-PA Author Manuscript

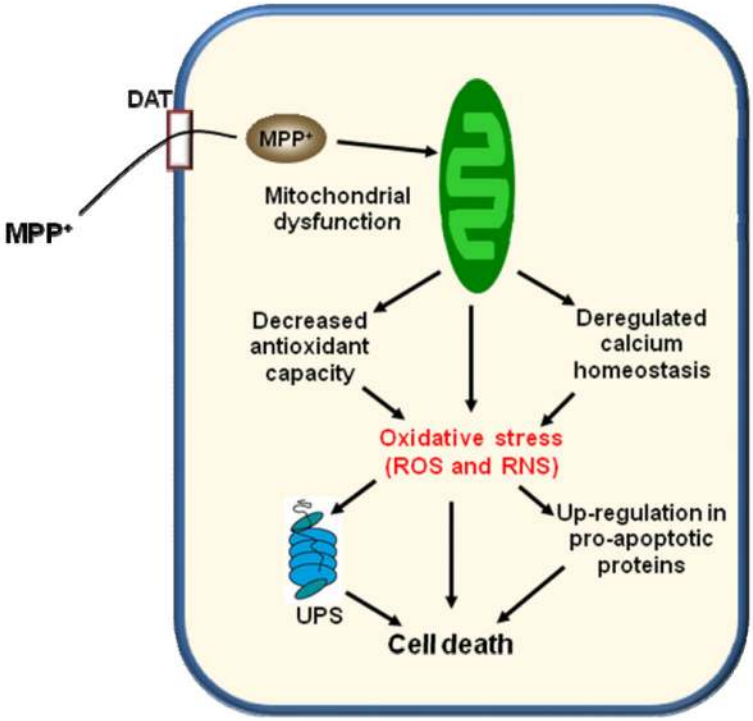

Figure 8.
A general mechanism of MPTP induced neurodegeneration.

NIH-PA Author Manuscript

NIH-PA Author Manuscript

NIH-PA Author Manuscript

Table 1

Number of peptides and proteins identified from the four brain regions.

Regions	Unique peptides	Unique proteins[a]	Significant proteins[b]
Striatum (Str)	23,894	3,928	192
Rest of Brain (ROB)	25,744	4,194	131
Cerebellum (CB)	24,084	4,171	133
Cortex (Cor)	22,940	3,515	124

[a] Proteins identified with more than 2 unique peptides.

[b] Proteins that show significant changes in abundance as induced by MPTP treatment.

NIH-PA Author Manuscript
NIH-PA Author Manuscript
NIH-PA Author Manuscript

J Proteome Res. Author manuscript; available in PMC 2010 April 26.

Table 2

Observed fold changes for selected proteins reported to be associated with PD.

IPI reference	Gene symbol	Protein name	Fold change[a]				References
			Str	ROB	CB	Cor	
IPI00226140.4	Maob[b]	amine oxidase b	2.5	−0.75	2	2	(42)
IPI00129191.1	Nos1	nitric-oxide synthase	−0.25	0.8	8	−0.11	(77)
IPI00111013.1	Ctsd[b]	cathepsin d	1.5	0.25	−0.083	−0.25	(22)
IPI00130992.1	Capns1[b]	calpain small subunit 1	2	−0.33	0.17	1.0	(22)
IPI00129577.1	Pdcd8[b]	programmed cell death protein 8	4.56	0	0.14	−1.0	(78)
IPI00331092.6	Rps4x	40s ribosomal protein s4	0	1.25	−0.125	0.83	(34)
IPI00400432.2	Eif4a2	eukaryotic initiation factor 4a-ii	0.55	0.86	−1.11	−0.375	(34)
IPI00227299.5	Vim[b]	Vimentin	1.0	0	−0.05	0.17	(34)
IPI00139518.3	Ubb	ubiquitin b	−1.0	2.4	0.575	−0.2	(34)
IPI00109727.1	Thy1	thy-1 membrane glycoprotein	0.63	−0.46	0.33	−0.31	(34)
IPI00119024.3	Arl6ip5	pra1 family protein 3	0.43	−0.4	−5	1.0	(34)
IPI00230124.4	Fabp3[b]	fatty acid-binding protein	1.0	2	4.56	1.0	(79)
IPI00113517.1	Ctsb[b]	cathepsin b	1.1	0.05	−0.8	−0.04	(48)
IPI00128567.1	Ache[b]	acetylcholinesterase	−1.33	0	0	0	(35)
IPI00626662.2	Aldh1a1[b]	retinal dehydrogenase 1	−1.22	−0.45	0.29	−1.0	(80) (22)
IPI00118787.1	Atp6v1d	vacuolar atp synthase subunit d	−0.57	−0.5	0.17	0.55	(22)
IPI00127598.1	Atpif1	atpase inhibitor	−1.0	−0.17	0.3	0.25	(22)
IPI00132531.1	Ndufb5	nadh dehydrogenase 1 beta	−0.8	−0.67	0.4	1.33	(22)
IPI00128023.3	Ndufs2	nadh-ubiquinone oxidoreductase 49 kda subunit	−0.27	0.05	−0.35	0.64	(22)
IPI00120232.1	Ndufs7	nadh-ubiquinone oxidoreductase 20 kda subunit	−0.33	0	−2	−0.33	(22)
IPI00131814.1	Ddc[b]	aromatic-l-amino-acid decarboxylase	−11.22	3.0	0	0	(37)
IPI00138131.1	Th[b]	tyrosine 3-monooxygenase	−4	−3.0	0	0	(38,39)
IPI00131614.1	Sncb	beta-synuclein	−0.6	0.32	0.12	0.71	(81,82)
IPI00131771.2	Cox6c[b]	cytochrome c oxidase polypeptide VIc	−1.25	0.67	−1.5	−0.11	(47)

NIH-PA Author Manuscript
NIH-PA Author Manuscript
NIH-PA Author Manuscript

IPI reference	Gene symbol	Protein name	Fold change[a]				References
			Str	ROB	CB	Cor	
IPI00119517.2	Cask	peripheral plasma membrane protein cask	−1.0	0.1	0.44	−1.375	(83)
IPI00756676.1	Bcas1	breast carcinoma amplified sequence 1	−0.67	0.09	−0.44	−0.4	(34)
IPI00755892.1	Hnrpdl	heterogeneous nuclear ribonucleoprotein D-like	0.083	0	−0.73	0.125	(34)
IPI00130840.6	Cope	coatomer subunit epsilon	0	−1.22	1.22	−5.67	(34)
IPI00480341.2	Gps1	cop9 signalosome	−0.67	0.5	1.0	−2.67	(34)
IPI00108143.1	Hnrph2	heterogeneous nuclear ribonucleoprotein h	−1.57	0.27	−0.13	−0.47	(22)
IPI00134621.2	Ran	gtp-binding nuclear protein ran	0.5	−0.14	0.25	−0.14	(34)
IPI00755653.1	Bcr	breakpoint cluster region	0.57	−0.14	−0.33	0	(34)
IPI00112414.1	Cse1l	exportin-2	−0.5	0.22	−0.4	0	(34)
IPI00119115.1	Atp6v1e1	vacuolar atp synthase subunit e	−0.17	−0.03	0.5	−0.065	(34)
IPI00308938.5	Capn2	calpain-2 catalytic subunit	3.44	0.2	0.33	1	(22)
IPI00331422.4	Cars	cysteinyl-trna synthetase	0.5	2	4.56	−0.25	(84)
IPI00135130.3	Slc1a4	neutral amino acid transporter a	−1	1.33	1	1.5	(85)
IPI00136912.1	Srm[c]	spermidine synthase	−4	0	0	0.2	(22)
IPI00129685.1	Tpt1[c]	translationally-controlled tumor protein	−1.5	0.29	−0.4	0.18	(34)
IPI00136967.2	Gria2[c]	glutamate receptor 2 precursor	−1.67	0.17	1.0	−0.86	(86)
IPI00224045.1	Chat[c]	choline o-acetyltransferase	2.5	0.11	0	0	(47)

[a] Significant fold changes were highlighted by gray color.

[b] Proteins known to be specifically changed in the nigrostriatal pathways due to the MPTP-treatment.

[c] Observed fold-changes of the protein disagree with previously reported changes.

NIH-PA Author Manuscript

NIH-PA Author Manuscript

NIH-PA Author Manuscript

Table 3

Significant proteins associated with different functional categories as shown in Figure 7.

IPI reference	Gene symbol	Protein name
Dopamine signaling		
IPI00118022.1	Ap2s1	AP-2 complex subunit sigma-1
IPI00131814.1	Ddc	aromatic-l-amino-acid decarboxylase
IPI00377680.3	Adcy2	adenylate cyclase 2
IPI00138131.1	Th	tyrosine 3-monooxygenase
IPI00228978.2	Cltb	clathrin light chain B
IPI00132410.1	Rab5a	RAS-related protein
IPI00223800.4	Pcbd1	pterin-4-alpha-carbinolamine dehydratase
IPI00108318.1	Ppp3cc	protein phosphatase 3
IPI00343381.5	Adcy5	adenylate cyclase 5
IPI00317759.4	Ppp2r2b	protein phosphatase 2A
IPI00118723.3	Ppp2r4	serine/threonine-protein phosphatase
IPI00169711.1	Maoa	amine oxidase A
IPI00226140.4	Maob	amine oxidase B
IPI00224697.1	Ppp2r5e	serine/threonine-protein phosphatase
IPI00119575.3	Prkar1a	protein kinase
IPI00126719.1	Ppp1r14a	protein phosphatase 1
Mitochondria dysfunction		
IPI00268145.4	Atp12a	potassium-transporting atpase alpha chain
IPI00378485.2	Atp1a4	sodium/potassium-transporting atpase alpha-4 chain
IPI00123704.1	Atp1b2	sodium/potassium-transporting atpase subunit beta-2
IPI00124221.1	Atp1b3	sodium/potassium-transporting atpase subunit beta-3
IPI00378453.3	Atp2b4	ATP2B4 protein
IPI00313475.1	Atp5c1	ATP synthase gamma chain
IPI00313841.1	Atp6v0d1	vacuolar ATP synthase subunit D
IPI00118787.1	Atp6v1d	vacuolar ATP synthase subunit D
IPI00315999.4	Atp6v1f	vacuolar ATP synthase subunit F
IPI00121443.1	Cox6a1	cytochrome C oxidase, subunit VI A
IPI00131771.2	Cox6c	cytochrome C oxidase polypeptide VIC
IPI00555023.1	Gstp2	glutathione S-transferase P 1
IPI00672194.2	LOC227112	ATP synthase, H+ transporting, mitochondrial F0 complex
IPI00125460.1	LOC674583	ATP synthase coupling factor 6
IPI00230715.4	Ndufa13	NADH dehydrogenase 1 alpha subunit 13
IPI00315302.4	Ndufa2	NADH dehydrogenase 1 alphasubunit 2
IPI00120212.1	Ndufa9	NADH dehydrogenase 1 alphasubunit 9
IPI00132390.4	Ndufb4	NADH dehydrogenase 1 beta subunit 4

NIH-PA Author Manuscript

NIH-PA Author Manuscript

NIH-PA Author Manuscript

IPI reference	Gene symbol	Protein name
IPI00132531.1	Ndufb5	NADH dehydrogenase 1 beta subunit 5
IPI00133215.2	Ndufb7	NADH dehydrogenase 1 beta subunit 7
IPI00387430.1	Ndufb8	NADH dehydrogenase 1 beta subunit 8
IPI00128023.3	Ndufs2	NADH-ubiquinone oxidoreductase
IPI00120232.1	Ndufs7	NADH-ubiquinone oxidoreductase
IPI00130460.1	Ndufv1	NADH-ubiquinone oxidoreductase
IPI00132762.1	Trap1	heat shock protein 75 kDa
IPI00132347.1	Uqcrb	ubiquinol-cytochrome C reductase binding protein
IPI00224210.4	Uqcrq	ubiquinol-cytochrome C reductase
Apoptosis and cell death		
IPI00123639.1	Calr	calreticulin
IPI00555023.1	Gstp2	glutathione S-transferase P 1
IPI00135475.2	Dbn1	drebrin
IPI00121013.1	Pea15	astrocytic phosphoprotein
IPI00278804.1	Scamp1	secretory carrier-associated membrane protein 1
IPI00131720.3	Cacnb4	calcium channel subunit beta-4
IPI00321942.4	Arfip2	arfaptin-2
IPI00129191.1	Nos1	nitric-oxide synthase
IPI00114368.2	Sec22b	vesicle-trafficking protein
IPI00116558.1	Rhog	RHO-related GTP-binding protein
IPI00130840.6	Cope	coatomer subunit epsilon
IPI00129577.1	Pdcd8	programmed cell death protein 8
IPI00761930.1	Prep	prolyl endopeptidase
IPI00227970.1	Exoc7	exocyst complex component 7
IPI00121623.1	Dynll1	dynein light chain 1
IPI00113517.1	Ctsb	cathepsin B
IPI00111013.1	Ctsd	cathepsin D
IPI00221613.4	Arf1	ADPribosylation factor 1
IPI00127942.3	Dstn	Destrin
IPI00112555.3	Gars	glycyl-trna synthetase
IPI00130992.1	Capns1	calpain small subunit 1
IPI00468140.2	Sorbs1	sorbin and sh3 domain-containing protein 1
IPI00323483.3	Pdcd6ip	programmed cell death 6-interacting protein
IPI00222557.4	S100b	protein s100-b
IPI00466424.4	Rab1	member ras oncogene family
IPI00320420.3	Clu	Clusterin
IPI00120193.1	Cdc42	cell division control protein 42
IPI00125861.2	Dlgh1	disks large homolog 1
IPI00125501.1	Epb4.1l3	band 4.1-like protein 3

NIH-PA Author Manuscript

NIH-PA Author Manuscript

NIH-PA Author Manuscript

IPI reference	Gene symbol	Protein name
IPI00467383.2	Cul3	cullin-3
IPI00125328.3	Epb4.9	Dematin
IPI00351827.5	Shank3	Shank3
IPI00120345.1	Gas7	growth-arrest-specific protein 7
IPI00270362.2	Rapgef4	RAP guanine nucleotide exchange factor 4
IPI00125880.1	Pacsin2	protein kinase c and casein kinase substrate in neurons protein 2
IPI00114380.1	Gstm5	glutathione S-transferase MU 5
IPI00129685.1	Tpt1	translationally-controlled tumor protein
IPI00119663.2	Mapk1	mitogen-activated protein kinase 1
IPI00420651.3	Ppp1r9b	neurabin-2
IPI00314153.4	Yars	tyrosyl-trna synthetase
IPI00321734.6	Glo1	lactoylglutathione lyase
IPI00137227.1	Rab2	RAS-related protein
IPI00229703.5	Vamp2	vesicle-associated membrane protein
IPI00626662.2	Aldh1a1	retinal dehydrogenase 1
IPI00469392.2	Rtn4	reticulon-4
IPI00130589.7	Sod1	superoxide dismutase
IPI00321922.2	Pacs1	phosphofurin acidic cluster sorting protein 1
IPI00750911.1	Myo5a	Myo5a protein
IPI00130368.4	LOC226472	glutathione S-transferase, mu 4
Calcium signaling		
IPI00459570.1	Tpm3	tropomyosin 3, gamma
IPI00108318.1	Ppp3cc	protein phosphatase 3
IPI00278611.5	Tpm3	tropomyosin alpha-3 chain
IPI00313475.1	Atp5c1	ATP synthase gamma chain
IPI00132526.1	Camk4	calcium/calmodulin-dependent protein kinase type IV
IPI00338309.3	Ryr2	cardiac Ca^{2+} release channel
Ubiquitin system		
IPI00402913.1	Ube2v2	ubiquitin-conjugating enzyme e2 variant 2
IPI00378681.4	Zubr1	CG14472-PA
IPI00323130.3	Tceb1	transcription elongation factor B polypeptide 1
IPI00108590.2	LOC639383	ubiquitin A-52 residue ribosomal protein
IPI00139518.3	Ubb	ubiquitin B
IPI00128760.1	Ube2l3	ubiquitin-conjugating enzyme
IPI00165854.3	Ube2n	ubiquitin-conjugating enzyme e2n
IPI00467383.2	Cul3	cullin-3
IPI00108388.1	Usp9x	ubiquitin carboxyl-terminal hydrolase FAF-x

NIH-PA Author Manuscript

NIH-PA Author Manuscript

NIH-PA Author Manuscript

IPI reference	Gene symbol	Protein name
IPI00462445.2	Nedd4	E3 ubiquitin-protein ligase